Selective inhibition of *Sarcocystis neurona* calcium-cependent protein kinase 1 for equine protozoal myeloencephalitis therapy

Kayode K. Ojo[a,*], **Sriveny Dangoudoubiyam**[b], **Shiv K. Verma**[c], **Suzanne Scheele**[d], **Amy E. DeRocher**[d], **Michelle Yeargan**[e], **Ryan Choi**[a], **Tess R. Smith**[a], **Kasey L. Rivas**[a], **Matthew A. Hulverson**[a], **Lynn K. Barrett**[a], **Erkang Fan**[f], **Dustin J. Maly**[g], **Marilyn Parsons**[d,h], **Jitender P. Dubey**[c], **Daniel K. Howe**[e,*], and **Wesley C. Van Voorhis**[a,h,*]

[a]Department of Medicine, Division of Allergy and Infectious Disease, Center for Emerging and Reemerging Infectious Disease (CERID), University of Washington, Seattle, WA 98109 USA

[b]Department of Veterinary Pathobiology, College of Veterinary Medicine and Biomedical Sciences, Texas A&M University, College Station, TX 77843 USA

[c]United States Department of Agriculture, Agricultural Research Service, Beltsville Agricultural Research Center, Animal Parasitic Diseases Laboratory, Beltsville, MD 20705 USA

[d]Center for Infectious Disease Research, Seattle, WA 98109 USA

[e]Department of Veterinary Science, University of Kentucky, Lexington, KY 40546 USA

[f]Department of Biochemistry, University of Washington, Seattle, WA 98195 USA

[g]Department of Chemistry, University of Washington, Seattle, WA 98195 USA

[h]Department of Global Health, University of Washington, Seattle, WA 98195 USA
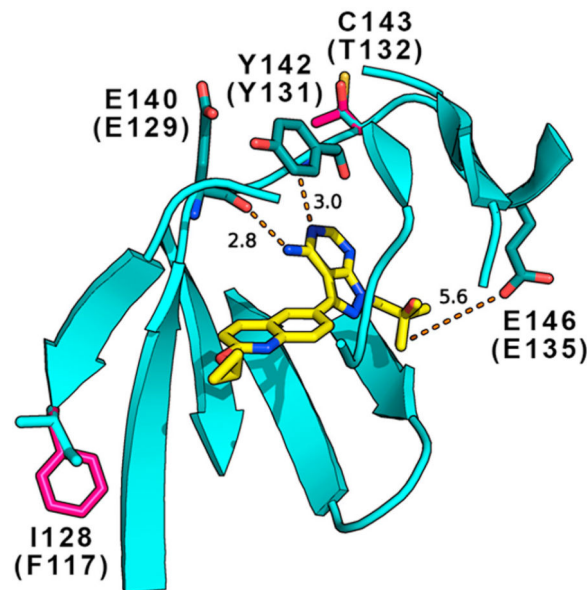
Abstract

Sarcocystis neurona is the most frequent cause of Equine Protozoal Myeloencephalitis (EPM), a debilitating neurological disease of horses that can be difficult to treat. We identified *Sn*CDPK1, the *S. neurona* homologue of calcium-dependent protein kinase 1 (CDPK1), a validated drug target in *Toxoplasma gondii*. *Sn*CDPK1 shares the glycine "gatekeeper" residue of the well-characterized *T. gondii* enzyme, which allows the latter to be targeted by bumped kinase inhibitors (BKIs). This study presents detailed molecular and phenotypic evidence that *Sn*CDPK1 can be targeted for rational drug development. Recombinant *Sn*CDPK1 was tested against four BKIs shown to potently inhibit both *T. gondii* (*Tg*)CDPK1 and *T. gondii* tachyzoite growth. *Sn*CDPK1 was inhibited by low nanomolar concentrations of these BKIs and *S. neurona* growth was inhibited at 40–120 nM concentrations. Thermal shift assays confirmed these BKIs bind CDPK1 in *S. neurona* cell lysates. Treatment with BKIs before or after invasion suggests that BKIs interfere with *S. neurona* mammalian host cell invasion in the 0.5–2.5 μM range but interfere with

[*]Corresponding authors. Kayode K. Ojo, Division of Allergy and Infectious Disease, Center for Emerging and Reemerging Infectious Disease (CERID), University of Washington, 750 Republican Street, E701, Box 358061, Seattle, WA 98109 USA.

intracellular division at 2.5 μM. In vivo proof-of-concept experiments were performed in a murine model of *S. neurona* infection. The experimental infected groups treated for 30 days with compound BKI-1553 (*n*=10 mice) had no signs of disease, while the infected control group had severe signs and symptoms of infection. Elevated antibody responses were found in 100% of control infected animals, but only 20% of BKI-1553 treated infected animals. Parasites were found in brain tissues of 100% of the control infected animals, but only in 10% of the BKI-1553 treated animals. The BKIs used in these assays have been chemically optimized for potency, selectivity and pharmacokinetic properties, and hence are good candidates for treatment of EPM.

Graphical Abstract

Keywords

Sarcocystis neurona; Equine Protozoal Myeloencephalitis; Calcium-dependent protein kinase 1; Gatekeeper residue; Drug target; Bumped kinase inhibitors

1. Introduction

Sarcocystis neurona, an apicomplexan parasite, is the most common cause of Equine Protozoal Myeloencephalitis (EPM), a debilitating neurological disease of horses. *Sarcocystis neurona* also causes clinical infection in a variety of domestic and wild animals, including fatal infections of marine mammals, notably on the western coast of the United States (Dubey et al., 2015a, b). Therapy for EPM initially employed inhibitors of folate synthesis and metabolism, given over a prolonged period of months (Dubey et al., 2015b). Ponazuril (Furr et al., 2001; MacKay et al., 2008), Diclazuril (Dubey et al., 2001a; Dirikolu et al., 2006), and Nitazoxanide (McClure and Palma, 1999) have been used more recently for the treatment of EPM, with variable success in eliminating clinical signs. Major challenges to current treatment options include incomplete response to therapy, relapse after therapy, the high cost of some therapies, and toxicity of some agents including effects such

as diarrhea and/or anemia (Dubey et al., 2001b, 2015a). Previous studies have shown that 55–70% of horses have some level of recovery after drug treatment but only 10–20% fully recover (MacKay, 2006). Up to 10% of treated horses relapse several months or years after the end of a successful initial response to therapy. The mechanism of relapses is not completely understood. However, regrowth of residual parasites after treatment and new *S. neurona* infection have both been suggested (Ellison and Lindsay, 2012). Thus, new approaches are needed to enhance outcomes.

Recently developed inhibitors of calcium-dependent protein kinases (CDPKs), have attracted great interest as targets for anti-apicomplexan drugs. By inhibiting certain highly conserved apicomplexan parasite CDPKs, bumped kinase inhibitors (BKIs) have shown broad ranging inhibitory effects in both in vitro and in vivo models of infections with *Toxoplasma gondii*, *Cryptosporidium parvum*, *Plasmodium* spp., *Neospora caninum* and *Theileria equi* (Murphy et al., 2010; Ojo et al., 2010, 2014a, b; Johnson et al., 2012; Castellanos-Gonzalez et al., 2013; Doggett et al., 2014; Hines et al., 2015; Huang et al., 2015; Vidadala et al., 2016). We have shown that inhibition of apicomplexan CDPK1 and subsequent interference with mammalian host cell invasion by BKIs was due to the atypical glycine "gatekeeper" residue in the ATP-binding site of the kinase as well as the overall topology of the ATP-binding site. Indeed, mammalian protein kinases in general have large gatekeeper residues, and mutation of the gatekeeper to glycine, coupled with BKI administration, allows selective "chemical-genetic" targeting of specific kinases in mammalian systems (Bishop et al., 1998). In this case, the BKIs do not target any mammalian protein kinases with any significant potency, but selectively target apicomplexan CDPK1s (Ojo et al., 2010; Wernimont et al., 2010).

We identified and sequenced a CDPK1 homologue (*Sn*CDPK1) in the *S. neurona* genome that also has a glycine gatekeeper residue. *Sn*CDPK1 and *T. gondii* (*Tg*)CDPK1 have approximately 87% overall amino acid sequence identity. Here, we further characterize BKIs for in vitro efficacy against *Sn*CDPK1 and *S. neurona* merozoites. Oral therapy with BKI-1553 eliminated *S. neurona* parasites from a murine model of sarcocystosis and the parasites did not recur up to 70 days after the end of treatment. Therefore, BKI-1553 is an important lead for the development of drugs for treatment of EPM.

2. Materials and methods

2.1. Compound synthesis

Bumped kinase inhibitors were synthesized as previously described (Murphy et al., 2010; Johnson et al., 2012; Huang et al., 2015; Vidadala et al., 2016). Purity of all compounds (>98%) was confirmed by reverse-phase HPLC and [^{1}H]- Nuclear magnetic resonance (NMR) spectroscopy.

2.2. Bioinformatics

The *S. neurona* homologue of *T. gondii* CDPK1 (**TgME49_301440**) was identified in an RNAseq dataset for the SN3.E1 strain of *S. neurona* (S. Dangoudoubiyam, D. Howe, unpublished data) using the TBLASTX and BLASTP tools on a local database of *S. neurona* sequences and later confirmed by amplification and sequencing of cDNA. Amino acid

identity values, sequence similarity and conserved domain searches were determined using the online tools (BLAST and CD-search) available at the National Center for Biotechnology Information (NCBI, USA).

2.3. Cloning, expression and purification of recombinant SnCDPK1

The complete coding region of *Sn*CDPK1 amplified from *S. neurona* SN3 strain cDNA was cloned into the AVA0421 expression vector as described (Ojo et al., 2011). Recombinant expression of *Sn*CDPK1 by auto-induction at 20°C was in *Escherichia coli* BL21(DE3) cells (Invitrogen, Carlsbad, CA, USA) as previously described (Studier, 2005; Ojo et al., 2011). Cell lysis buffer for protein extraction contained 25 mM HEPES (pH 7.25), 500 mM NaCl, 5% glycerol, 2 mM DTT, 10 mg of lysozyme with 30 mM imidazole. Soluble recombinant *Sn*CDPK1 was purified by immobilized metal-affinity chromatography in a Ni–NTA (Qiagen, Valencia, CA, USA) column as described earlier (Ojo et al., 2011). Purified enzyme for activity and inhibitor screening assays was stored at −20°C in 50% glycerol, 12.5 μM HEPES (pH 7.5), 250 μM NaCl, 0.5 μM DTT, 0.0125% sodium azide and 1X protease inhibitor (Roche, Indianapolis, IN, USA) (Ojo et al., 2011).

2.4. TgCDPK1 antibody production and analysis

Recombinant *Tg*CDPK1 protein, expressed and purified from a 1.43 kb DNA fragment encoding amino acid residues 30–507 (Ojo et al., 2010), was used as antigen for anti-*Tg*CDPK1 production. The rabbit polyclonal antibody was produced at R&R Research, LLC (Stanwood, WA, USA) by injecting two rabbits with 0.5 mg of *Tg*CDPK1 initial dose per animal. Five booster doses were administered at 0.25 mg per boost over a period of 3.5 months and serum was obtained 3 months later. Antibody specificity and ability to detect *Sn*CDPK was analyzed by western blotting using purified recombinant *Sn*CDPK1, *T. gondii* tachyzoites and a human foreskin fibroblast cell line as host cell control (Supplementary Fig. S1A). Further serial dilution of cells was used to determine the linearity of antibody response. Antisera from both rabbits detected the purified CDPK1 antigen on western blots at 1:100,000 dilutions (Supplementary Fig. S1A) and a slightly larger band in *T. gondii* tachyzoites as expected since the recombinant antigen had the first 29 N-terminal amino acid residues deleted relative to the wild-type enzyme (predicted molecular weight of 57.26 versus 54.73 kDa). Serial *T. gondii* parasite dilutions show a linear relationship between sample load and signal strength in the immunoblot (Supplementary Fig. S1B). The anti-*Tg*CDPK1 serum used in this study recognized a band in *S. neurona* lysates which was slightly larger than *Tg*CDPK1 as expected given the predicted molecular weight of 58.84 kDa versus 57.26 kDa (Supplementary Fig. S1C).

2.5. Thermal shift assays

Thermal stability of recombinant *Sn*CDPK1 in the presence or absence of inhibitors was determined in a 96-well format as previously described (Crowther et al., 2009) using Applied Biosystems StepOnePlus™ Real-Time PCR System (Carlsbad, CA, USA). Each assay well contained a reaction mixture of 0.1 mg/mL of *Sn*CDPK1 enzyme, 20 μM of each inhibitor when present, and 5% DMSO. Internal control comprising of *Sn*CDPK1 and 5% DMSO was included in each assay plate. All assays were performed independently three

times. Subsequent analysis and calculation of melting temperature values were performed using Graphpad® Prism software (GraphPad Software, San Diego, CA, USA).

The cell lysate thermal shift assay (TSA) was a modification of a previously described procedure (Martinez Molina et al., 2013). *Sarcocystis neurona* schizonts or merozoites cells were harvested, washed in PBS, counted and resuspended in TSA buffer containing 25 mM Tris HCl (pH 7.4), 2 mM DTT, 10 mM $MgCl_2$, 1 mM $CaCl_2$, phosphatase and Halt protease inhibitor cocktail (Thermo Scientific, USA). Cells were lysed by three freeze-thaw cycles using liquid nitrogen. Cell lysates were clarified at 16,100 *g* for 25 min at 4°C. Thermal stabilization of *Sn*CDPK1 in the clarified cell lysate was tested at seven temperature (66°C, 62°C, 58°C, 54°C, 50°C, 46°C, and 42°C) points in duplicate per compound in a reaction volume of 20 μL at a BKI final concentration of 2 μM, and 0.5% DMSO. Samples were placed in a PCR machine (MJ Research PTC-100, USA) and after 3 min at the temperature indicated above; they were centrifuged as described above to remove aggregates of denatured proteins. Supernatants containing soluble protein (10 μL) were mixed with 10 μL of 2x SDS-PAGE sample buffer freshly made with 4% 2-mercaptoethanol. Proteins from cell lysate equivalent to $2x10^6$ cells/lane (8 μL of sample mixture) were separated by SDS-PAGE before western blot using anti-*Tg*CDPK1 (1:50,000) as probe followed by secondary goat anti-rabbit IgG(H+L) coupled to IRDye 680 (1:20,000) (LI-COR, Lincoln, NE, USA). After scanning on a LI-COR Odyssey Imaging System, the data was imported into LICOR Image Studio Software. Background correction was applied (median background, right/left segment option). Each compound was tested in duplicate (data points were averaged for calculations of melting temperatures (T_m) in at least two experiments). The solvent control was similarly tested in duplicate, and repeated three times to yield an average T_m value used for the final calculation of the thermal shift. The percentage of CDPK1 (S) remaining soluble at each temperature (T) was calculated from the averaged replicates, using the highest signal for soluble CDPK1 as 100% (usually the 37°C point). The T_m for each compound in each experiment was calculated using the following equation where T_1 and T_2 are the temperatures flanking the estimated Tm, and S_1 and S_2 are corresponding soluble CDPK1: $[(S_1-0.5)/(S_1-S_2) \times (T_2-T_1)] + T_1$. The thermal shift was defined as the T_m (compound)-T_m (DMSO).

2.6. SnCDPK1 kinase activity assays

Measurement of enzyme activity of recombinant *Sn*CDPK1 and inhibition of its protein kinase phosphorylation properties by small molecule inhibitors was carried out in a non-radioactive assay as described earlier (Ojo et al., 2014b). This assay measures changes in initial ATP concentration after *Sn*CDPK1 phosphorylation of biotinylated peptide substrate PLARTLSVAGLPGKK (American Peptide Company, Inc. Sunnyvale, CA, USA) via luminescence using the Kinase-Glo® luciferase reagent (Promega, Madison, WI, USA). The assay buffer is composed of 1 mM EGTA (pH 7.2), 10 mM $MgCl_2$, 20 mM HEPES pH 7.5 (KOH), 0.1% BSA and enzyme activation reagent containing 2 mM $CaCl_2$. The reaction mixture containing 3 nM of recombinant *Sn*CDPK1, 20 μM peptide substrate and 10 μM ATP was incubated at 30°C. The reaction was terminated after 90 min incubation with the addition of 5 mM EGTA. Each experiment included reactions without peptide substrate as controls and no ATP consumption was noted without substrate.

2.7. Parasite growth assays

Five previously characterized BKIs (1294, 1266, 1517, 1553 and 1561) were selected for this study. Four of these (1294, 1517, 1553 and 1561) have previously been chemically optimized with functional groups needed to improve potency, selectivity and pharmacokinetic properties while BKI-1266 was chosen as a negative control (Doggett et al., 2014; Ojo et al., 2014b; Huang et al., 2015; Vidadala et al., 2016). Bovine turbinate (BT) cells maintained in RPMI 1640 medium supplemented with 10% fetal bovine serum, 2 mM sodium pyruvate, and Pen/Strep Fungizone (BioWhittaker, Walkersville, MD, USA) were seeded into 96-well plates. After 24 h, medium was replaced with that containing a serial concentration of BKI compounds. Yellow fluorescent protein (YFP)-expressing *S. neurona* strain F9F merozoites were used according to procedures described previously (Gaji et al., 2006). Freshly released F9F merozoites purified from cell debris were resuspended in culture medium without phenol red, and BT cell monolayers were inoculated with 4×10^4 parasites per well, eight wells per treatment. BKIs were added to BT host cells at the time of inoculation except as indicated. Extracellular parasites were washed out after 2 hours, and then drug was again added to the cultures for the duration of the growth assay. The plates were incubated at 37°C for 4 days. Fluorescence was measured daily using a Synergy H1 plate reader (BioTek, Winooski, VT, USA).

2.8. Mouse infection experiments

All investigations reported here were approved by the institutional animal care and use protocol committee (IACUC) guidelines of the US Department of Agriculture. IFNγ gene knockout (IFNγ-KO) mice, known to be susceptible to *S. neurona* infection, were purchased (Jackson Laboratory, Bar Harbor, ME, USA). The animals were housed in plastic cages with corn cob bedding. All animals before and during experimental infections were placed in a controlled climate and photoperiod (23 ± 2°C; 60% relative humidity (RH) and 12 h light-dark cycles) and fed rodent laboratory chow (ENVIGO, Teklad global 19% protein extruded rodent diet, Madison, WI, USA) and water ad libitum. Healthy, normal male and female IFNγ-KO mice of 3–4 months old (weight 20–30 g) were used in the present study and observed daily for signs of illness. *Sarcocystis neurona* strain SN 37R cultured in African green monkey kidney (CV-1) cells was used for the mouse infection experiment and evaluation of anti-parasitic efficacy of BKI-1553 in vivo (Dubey et al., 2015a). Each animal was inoculated with 20,000 merozoites s.c. (Table 1). Compound BKI-1553 at 0.02 mg/mL was dissolved in water having 0.5% saccharine using magnetic stirring at 60°C and offered to the mice as drinking water on the day after infection and continued for 30 days (Table 1). Control mice were given plain water for drinking throughout the duration of the experiment. The calculated daily dose of BKI-1553 was approximately 4.8 mg/kg based on a 25 g average mouse weight and 6 mL drinking volume/day. Midway through the experiment, mice from experimental groups #7 and #8 were bled from the tail (approximately 25 μL) and heparinized plasma prepared at 16:00 h with five of the mice also sampled at 08:00 h. The plasma was assayed for BKI-1553 levels by quantitative LC-MS as previously described (Ojo et al., 2014a; Vidadala et al., 2016). Animals were euthanized and brains of medicated and challenged IFNγ-KO mice that survived were sub-inoculated into IFNγ-KO mice to detect infections that could have been missed by histopathology and serological examinations. Blood samples were collected for serology at the time of death. To assess

infection, sera were tested with an ELISA based on *S. neurona* surface antigens (Yeargan et al., 2015) and using goat anti-mouse secondary reagent to detect antibodies against *S. neurona*. Portions of heart, lung, spleen, tongue, eye, brain, kidney, liver, intestine and muscles were fixed in 10% buffered neutral formalin for immunohistochemical examination. Fixed tissues were cut into sections (2.5 x 0.7 cm) placed in cassettes, embedded in paraffin and sectioned at 5 μM thickness. Paraffin sections were reacted with anti-*S. neurona* serum prepared from a rabbit injected with culture-derived *S. neurona* merozoites as described by Dubey et al. (1999). The specificity of the *S. neurona* antiserum has been described previously (Dubey and Hamir, 2000).

3. Results

3.1. SnCDPK1 and TgCDPK1 homology

Blast searches of an RNA-Seq dataset for *S. neurona* using *Tg*CDPK1 as the query retrieved a transcript encoding a 524 amino acid *Sn*CDPK1 homologue. Later, two complete genome sequences of *S. neurona* (SN3.E1 strain (SN3_02800495) and the SOSN1 strain (SRCN_3314_SN1)) were added to ToxoDB (www.toxodb.org/toxo/), but the exon predictions were different from those we had identified from the RNA-Seq data. We confirmed our prediction by amplification from *S. neurona* SN3 strain cDNA and sequencing of the cloned product (Supplementary Fig. S2).

Alignment of *Tg*CDPK1 (GenPept accession number **AAG53993.1**) with *Sn*CDPK1 revealed 87% overall sequence identity, increasing to 96% in the active site residues that directly or indirectly contact ATP and 99% identity in the residues that contact BKIs shown in the boxes in Fig. 1A. BLAST (*Sn*CDPK1 versus *T. gondii*) showed that the next best hit for *Sn*CDPK1 is *T. gondii* CDPK3 (GenBank Sequence ID: **XP_002370358.1**) with an overall sequence identity of 59%. The next best hit to this was CDPK2A (GenBank Sequence ID: **EPT29907.1**) with 44%. The data suggests that the two enzymes (*Sn*CDPK1 and *Tg*CDPK1) are homologues as further reinforced by the fact that the putative *Sn*CDPK1 sequence is syntenic with *Tg*CDPK1. A hypothetical homology model of the *Sn*CDPK1 amino acid residues predicted to contact BKIs is super-imposed on *Tg*CDPK1-1561 crystal complex (PDB accession code: **4TZR**) to display their spatial orientation and interaction with the inhibitor is presented in Fig. 1. The model and figure were generated using PyMOL software (Delano Scientific, Palo Alto, CA, USA). Hypothetical modeling of *Sn*CDPK1interaction with BKI-1561 based on the starting crystal complex 4TZR was straightforward with >95% similarity and no insertions or deletions in the ATP binding site. Only two amino acid residue, I128 (F117) and C143 (T132), changes within 8Å of the bound BKI were effected using the PyMOL mutagenesis wizard tool. The rotamers were chosen based on the best fits and orientations. Similar hydrogen-bonding contacts from the backbone carbonyl of *Sn*CDPK1 E140 (*Tg*CDPK1 E129) and the backbone nitrogen of Y142 (Y131) to the exocyclic amine and adjacent endocyclic nitrogen of the pyrazolopyrimidine ring of 1561 could be observed in both enzymes. In both complexes, the 2-methylpropan-2-ol R2 group of 1561 extends into their ribose pockets and makes a hydrogen bond with the E146 (E135) side chain carboxylate as previously observed for a piperidine R2 ring of BKI (Johnson et al., 2012). Two amino acid residues, I128 (F117) and

C143 (T132), within the BKI binding region differ between *Sn*CDPK1 and *Tg*CDPK1. These are both predicted by the model to contribute backbone atoms to the binding site but have very limited effects on BKI inhibition. It was therefore logical to test BKIs that had been designed to inhibit *Tg*CDPK1 for their ability to inhibit *Sn*CDPK1. *Sn*CDPK1 was cloned and expressed in *E. coli*, and analyzed by thermal shift ligand assays and BKI inhibition.

3.2. SnCDPK1 interacts with BKIs: thermal shift and BKI inhibition

The thermal stability of recombinant *Sn*CDPK1 and *Tg*CDPK1 was assessed by establishing their T_m via TSAs. The results were compared with the same protocol conducted in the presence of 20 μM BKI. Significant shifts in T_m were observed in the presence of BKI compounds 1294, 1517, 1553 and 1561 (Table 1, Figs. 2, 3) while very little change was observed for compound 1266 (Fig. 2). This thermal stabilization T_m correlated excellently with data obtained from inhibition of phosphorylation activity for each of the selected BKIs. The inhibition concentration to give 50% reduction in enzyme activity (IC_{50}) was measured as less than 10 nM for BKIs 1294, 1517, 1553, 1561 and >2 μM for 1266 (Table 1). Compound 1266 does not inhibit *Tg*CDPK1, so it was not surprising that it was also inactive against *Sn*CDPK1.

3.3. Cell lysate thermal shift

Cell lysate TSAs can help determine if compounds are binding to the targeted protein in a complex mixture of proteins, such as the constellation of ATP-binding proteins that reside in the cell. In the absence of ligand, 50% of *Sn*CDPK1 enzyme in cell lysates denatured at 47.4°C (T_m) and became removable by centrifugation. Compound 1266, which was inactive in the direct enzyme activity and growth assays, did not shift the T_m (Fig. 4). In contrast, there was a shift in T_m for the test compounds compared with the controls (Fig. 4). Active *Sn*CDPK1-inhibitory BKIs 1294, 1517, and 1553 stabilized the CDPK1 enzyme in the cell lysate, showing a shift of 2.7°C (1294), 4.1°C (1553), and 8.0°C (1517), with the shift in T_m trending towards inverse correlation with the IC_{50}s for enzyme inhibition, although our data do not allow calculation of statistical significance. This suggests the more potent BKIs preferentially bound to the CDPK1 in complex mixtures approximating the cellular proteome. In general, the amount of thermal shift seen was smaller in cell lysates than seen with the recombinant *Sn*CDPK1 treated with the same BKIs. This could be due to differences in compound and protein concentrations between the two assays as well as interactions (specific or non-specific) with other proteins in the cell lysate assay.

3.4. Sarcocystis neurona inhibition in cell culture

The effects of BKIs on *S. neurona* invasion and growth in mammalian cells were assessed in cell culture. All four optimized BKIs with low nanomolar IC_{50}s against recombinant *Sn*CDPK1 kinase activity also inhibited *S. neurona* merozoite proliferation in vitro with EC_{50} values as low as 42 nM for BKI-1517 and 1553, and up to 128 nM for BKI-1561 (Table 1). There was a trend towards a correlation between the IC_{50} of *Sn*CDPK1 enzyme and the EC_{50} of *S. neurona* in tissue culture. At 0.5–2.5 μM concentrations, the BKIs were more effective when added at the time of inoculation versus 2 h later (Fig. 5), suggesting that, as for *T. gondii*, BKIs inhibit *S. neurona* invasion into host cells. However, effects on

intracellular parasite proliferation became evident at 2.5 μM BKI concentration. At the 2.5 μM BKI concentration, the parasites proceeded through endopolygeny (albeit much slower than untreated parasites), but they appeared to arrest just prior to the cytokinesis that forms the daughter merozoites. Host cells contained late-stage schizonts that had not divided into daughter merozoites at days 8–9 p.i., well beyond when the untreated parasites had lysed the host cell monolayer (day 5; data not shown).

3.5. In vivo treatment of S. neurona-infected mice

BKI-1553 was chosen for *S. neurona* therapy of mice because it had superior oral bioavailability and long exposure after dosing, was known to penetrate the CNS, had excellent safety parameters (Vidadala et al., 2016), and good efficacy against *S. neurona* in vitro. Preliminary experiments with BKI-1553 demonstrated that mice could be exposed by oral gavage to multi-micromolar BKI blood levels for 6 weeks without evident toxicity. A pilot pharmacokinetic study in uninfected mice showed that delivery of BKI-1553 (0.02 mg/mL) in drinking water yielded steady state plasma concentrations between 3.9 and 6.1 μM for 1 week, as measured twice per day (data not shown).

In vivo proof-of-concept experiments performed in a murine IFNγ-KO model of *S. neurona* infection investigated whether BKI-1553 has potential as a therapeutic for EPM. Animals in BKI-1553 treated experimental (challenged) groups and BKI-1553 control (non-challenged) groups were healthy without any evidence of toxicity as inferred from cage-side observations of gross clinical signs and from histopathology. The challenged and non-treated control groups (#3, #4) developed neurological signs resulting in death or the need for euthanasia between 39–70 days p.i. (Table 2). High anti-*S. neurona* titers (1:8000 and up) were detected in their blood and *Sarcocystis* schizonts and merozoites were found in their brains, particularly the cerebellum (Table 2). In the BKI-1553 treated experimental groups, the plasma levels of BKI-1553 were found to be between 2.5 and 9.9 μM (average concentration 6 μM) in the 10 mice tested after steady state had been achieved, and there was not much diurnal variation in the five mice tested both in the morning and evening (Table 3). Eight of 10 mice in the experimental groups (#7, #8) inoculated with *S. neurona* and subsequently treated with BKI-1553 were seronegative for antibodies, and parasites were not found in their brain tissues (Table 2). Two mice, one from each of the challenged and treated groups (#7, #8), developed modest anti-*S. neurona* titers (1:1000 and 1:2000), but did not show any clinical signs even at the termination of the experiment (70 days p.i.). Parasites were detected in the brain of the seropositive mouse F of group #7 (Table 3) by immunohistological examination, but not in the seropositive mouse in group #8. As well, sub-inoculation of pooled brain homogenates from group #7 resulted in the recipient IFNγ-KO mouse becoming seropositive and developing clinical *S. neurona* infection. However, *S. neurona* infection did not develop in recipient IFNγ-KO mice that were sub-inoculated with pooled brain homogenates from the mice in group #8. Thus, in conclusion, it appears that BKI-1553 had no ill effects on the mice and it led to clearance of *S. neurona* infection in 90% of mice.

4. Discussion

Taken as a whole, the data presented in this paper support CDPK1 as a promising drug target for *S. neurona* therapeutics. First, the structure and active site of *Sn*CDPK1 is highly similar to that of *T. gondii* CDPK1, suggesting that the BKIs designed to potently and selectively inhibit *Tg*CDPK1 would be active against *Sn*CDPK1. Second, recombinant *Sn*CDPK1 enzyme inhibition and thermal shift results show that the four selected BKIs, which are strong inhibitors of *Tg*CDPK1, indeed bind to and inhibit *Sn*CDPK1. Third, the BKIs inhibited *S. neurona* cell growth with EC_{50} values that trended towards correlation with their IC_{50} values against recombinant *Sn*CDPK1. Fourth, a control BKI (1266), which is highly related chemically to the other three BKIs tested (1294, 1553 and 1561) but lacks *Tg*CDPK1 inhibitory activity, failed to inhibit or bind *Sn*CDPK1 and had no discernable activity against *S. neurona* in cell culture. Fifth, exposing cell lysates to the BKIs led to thermal stabilization of CDPK1, suggesting that the BKIs are binding to *Sn*CDPK1 in complex *S. neurona* cellular lysates at therapeutic concentrations and supports the contention that *Sn*CDPK1 is the target of BKI inhibition. It should be noted that there was an order of magnitude less compound used in the cell lysate assay compared with the purified recombinant enzyme assay. This is because the goals of the experiments were different. For the purified protein assay, it was simply looking for interaction with high to saturating amounts of reagents. For the cell lysate assay, it was finding a concentration that could be effective without being high to the point of having off-target effects on the cells. The choice of 2 µM for lysate was an estimation at the high end of what might be happening with drug treatment. Finally, administration of BKI-1553 to mice one day after challenge with *S. neurona* led to good clinical outcomes compared with non-treated mice, which had progressive infection and became uniformly moribund. Serological analysis suggests attenuated infection in most mice treated with BKI-1553, and histological examination and tissue sub-inoculations revealed no *S. neurona* in 90% of these mice.

These data showed that BKIs that inhibited *Sn*CDPK1 reduced parasite invasion and growth. While it is not definite that *Sn*CDPK1 is the primary target for the BKIs, chemical-genetic evidence has been obtained for *T. gondii* using genetic manipulation. Purified *Tg*CDPK1 (G128M), which has a methionine substituted for the glycine gatekeeper residue, is resistant to inhibition by 1294, 1553 and 1561 (Johnson et al., 2012; Vidadala et al., 2016). In the *T. gondii* cellular assay, when we over-expressed *Tg*CDPK1 (G128M), there was at least a 10-fold shift in resistance to BKIs 1294, 1553 and 1561, which was not observed upon over-expression of the wild-type allele. Basic molecular genetic capabilities are available for *S. neurona*, but the comparable experiment has not been attempted in this parasite.

Additional evidence that BKIs act through *Sn*CDPK1 comes from studies on the timing of inhibitor delivery. In *T. gondii*, CDPK1 signaling is responsible for regulating gliding motility and host cell entry and egress (Lourido et al., 2010, 2012). For both *S. neurona* and *T. gondii*, BKIs added at the time of infection in vitro are more potent than if BKIs are added later. These data are again compatible with the hypothesis that the BKIs act via *Sn*CDPK1. However, we observed that at higher BKI drug concentrations, the parasites proceeded through endopolygeny but arrested prior to cytokinesis. This may suggest that higher concentrations of BKIs act on a second target that is related to cell replication and division.

Similar observations have been described when cultures of *N. caninum* tachyzoites were treated with high concentration of BKI-1294 (Ojo et al., 2014b). We looked for other protein kinases with small gatekeeper residues that BKIs may target in the *S. neurona* genome. There were no protein kinases with glycine or alanine gatekeeper residues that we could find. However, two protein kinase open reading frames with serine gatekeeper residues in the *S. neurona* kinome (as derived from Sngenome) that BKIs could potentially inhibit are found in scaffold_13_1057269- 1066648 (a calmodulin-domain protein kinase) and a CMGC kinase, mitogen-activated protein kinase 1 (MAPK-1) like enzyme (**SN3_00202170**). However, in previous studies we showed that the topology of the active site of CDPK1 was as important as the gatekeeper residue in BKI targeting, thus we are uncertain if any of these kinases with serine gatekeepers would be targeted by our BKIs.

The early timing in vitro for potent inhibition does not impede BKIs from being effective therapy in vivo once infection is established since cycles of invasion and egress are needed for pathogenesis. In this report, BKIs were effective in eradicating *S. neurona* infection that was established 1 day prior to the initiation of therapy. In a previous publication, we have shown BKIs effectively eradicated *T. gondii* infection after 2 days of established infection (Doggett et al., 2014). Since EPM is most often diagnosed after the acute phase of infection, it remains to be seen if BKIs can effectively reduce signs and symptoms of EPM.

BKIs may improve current therapy for EPM, which is challenged by incomplete response to therapy, relapse and high cost. Currently available drugs for EPM therapy, such as Ponazuril (Furr et al., 2001; MacKay et al., 2008) and Diclazuril (Dubey et al., 2001a; Dirikolu et al., 2006), have been shown to clinically benefit horses with EPM. Thus, the best way to demonstrate the utility of BKIs for the therapy of EPM would be to perform a randomized trial of BKIs and either Ponazuril or Diclazuril in horses with early EPM. In preparation for such a trial, pharmacokinetic studies would be performed to establish a formulation and route of administration of BKIs that gives sufficient exposure in horses to expect therapeutic success. We have already established outstanding oral pharmacokinetics for BKIs 1294, 1553 and 1517 in newborn calves (unpublished data). Thus, our prediction would be that the BKI compounds could be delivered orally to horses with EPM with good exposures in the range that would be expected to be effective in inhibiting the growth of *S. neurona*. The BKIs have demonstrated outstanding in vitro safety parameters in rodents, so we do not anticipate safety issues with horses. Unfortunately BKI-1294 has recently been shown to have hERG inhibition (Ojo et al., 2014a), associated with long QT syndrome in humans and potentially fatal arrhythmias (Pollard et al., 2010). This may be an issue in the therapy of horses, for they have slow resting heart rates (Marr et al., 1995), and might be susceptible to long QT associated arrhythmias. For that reason, BKI-1553 and BKI-1517 are more appealing agents for EPM therapy in horses because of their lack of hERG inhibition (Vidadala et al., 2016). Since BKI-1553, compared with BKI-1517 has decreased clearance in most species, larger exposure and greater CNS distribution, it might be the better BKI to test first in EPM horses.

Supplementary Material

Refer to Web version on PubMed Central for supplementary material.

Acknowledgments

References

Bishop AC, Shah K, Liu Y, Witucki L, Kung C, Shokat KM. Design of allele-specific inhibitors to probe protein kinase signaling. Curr Biol. 1998; 8:257–266. [PubMed: 9501066]

Castellanos-Gonzalez A, White AC, Ojo KK, Vidadala RS, Zhang Z, Reid MC, Fox AM, Keyloun KR, Rivas K, Irani A, Dann SM, Fan E, Maly DJ, Van Voorhis WC. A novel calcium-dependent protein kinase inhibitor as a lead compound for treating cryptosporidiosis. J Infect Dis. 2013; 208:1342–1348. [PubMed: 23878324]

Crowther GJ, Napuli AJ, Thomas AP, Chung DJ, Kovzun KV, Leibly DJ, Castaneda LJ, Bhandari J, Damman CJ, Hui R, Hol WG, Buckner FS, Verlinde CL, Zhang Z, Fan E, van Voorhis WC. Buffer optimization of thermal melt assays of *Plasmodium* proteins for detection of small-molecule ligands. J Biomol Screen. 2009; 14:700–707. [PubMed: 19470714]

Dirikolu L, Karpiesiuk W, Lehner AF, Hughes C, Woods WE, Harkins JD, Boyles J, Atkinson A, Granstrom DE, Tobin T. New therapeutic approaches for equine protozoal myeloencephalitis: pharmacokinetics of diclazuril sodium salts in horses. Vet Ther. 2006; 7:52–63. 72. [PubMed: 16598684]

Doggett JS, Ojo KK, Fan E, Maly DJ, Van Voorhis WC. Bumped kinase inhibitor 1294 treats established *Toxoplasma gondii* infection. Antimicrob Agents Chemother. 2014; 58:3547–3549. [PubMed: 24687502]

Dubey JP, Mattson DE, Speer CA, Baker RJ, Mulrooney DM, Tornquist SJ, Hamir AN, Gerros TC. Characterization of a *Sarcocystis neurona* isolate (SN6) from a naturally infected horse from Oregon. J Eukaryot Microbiol. 1999; 46:500–506. [PubMed: 10519218]

Dubey JP, Hamir AN. Immunohistochemical confirmation of *Sarcocystis neurona* infections in raccoons, mink, cat, skunk, and pony. J Parasitol. 2000; 86:1150–1152. [PubMed: 11128499]

Dubey JP, Fritz D, Lindsay DS, Shen SK, Kwok OC, Thompson KC. Diclazuril preventive therapy of gamma interferon knockout mice fed *Sarcocystis neurona* sporocysts. Vet Parasitol. 2001a; 94:257–264. [PubMed: 11137273]

Dubey JP, Lindsay DS, Saville WJ, Reed SM, Granstrom DE, Speer CA. A review of *Sarcocystis neurona* and equine protozoal myeloencephalitis (EPM). Vet Parasitol. 2001b; 95:89–131. [PubMed: 11223193]

Dubey, JP.; Calero-Bernal, R.; Rosenthal, BM.; Speer, CA.; Fayer, R. Sarcocystosis of Animals and Humans. Second. CRC Press, Taylor & Francis Group, USA; 2015a.

Dubey JP, Howe DK, Furr M, Saville WJ, Marsh AE, Reed SM, Grigg ME. An update on *Sarcocystis neurona* infections in animals and equine protozoal myeloencephalitis (EPM). Vet Parasitol. 2015b; 209:1–42. [PubMed: 25737052]

Ellison S, Lindsay DS. Decoquinate Combined with Levamisole Reduce the Clinical Signs and Serum SAG 1, 5, 6 Antibodies in Horses with Suspected Equine Protozoal Myeloencephalitis. Int. J. Applied Res Vet Med. 2012; 10:1–7.

Furr M, Kennedy T, MacKay R, Reed S, Andrews F, Bernard B, Bain F, Byars D. Efficacy of ponazuril 15% oral paste as a treatment for equine protozoal myeloencephalitis. Vet Ther. 2001; 2:215–222. [PubMed: 19746664]

Gaji RY, Zhang D, Breathnach CC, Vaishnava S, Striepen B, Howe DK. Molecular genetic transfection of the coccidian parasite *Sarcocystis neurona*. Mol Biochem Parasitol. 2006; 150:1–9. [PubMed: 16844242]

Hines SA, Ramsay JD, Kappmeyer LS, Lau AO, Ojo KK, Van Voorhis WC, Knowles DP, Mealey RH. *Theileria equi* isolates vary in susceptibility to imidocarb dipropionate but demonstrate uniform in vitro susceptibility to a bumped kinase inhibitor. Parasit Vectors. 2015; 8:33. [PubMed: 25600252]

Huang W, Ojo KK, Zhang Z, Rivas K, Vidadala RS, Scheele S, DeRocher AE, Choi R, Hulverson MA, Barrett LK, Bruzual I, Siddaramaiah LK, Kerchner KM, Kurnick MD, Freiberg GM, Kempf D, Hol WG, Merritt EA, Neckermann G, de Hostos EL, Isoherranen N, Maly DJ, Parsons M, Doggett JS, Van Voorhis WC, Fan E. SAR Studies of 5-Aminopyrazole-4-carboxamide Analogues as Potent and Selective Inhibitors of *Toxoplasma gondii* CDPK1. ACS Med Chem Lett. 2015; 6:1184–1189. [PubMed: 26693272]

Johnson SM, Murphy RC, Geiger JA, DeRocher AE, Zhang Z, Ojo KK, Larson ET, Perera BG, Dale EJ, He P, Reid MC, Fox AM, Mueller NR, Merritt EA, Fan E, Parsons M, Van Voorhis WC, Maly DJ. Development of *Toxoplasma gondii* calcium-dependent protein kinase 1 (TgCDPK1) inhibitors with potent anti-toxoplasma activity. J Med Chem. 2012; 55:2416–2426. [PubMed: 22320388]

Lourido S, Shuman J, Zhang C, Shokat KM, Hui R, Sibley LD. Calcium-dependent protein kinase 1 is an essential regulator of exocytosis in *Toxoplasma* . Nature. 2010; 465:359–362. http://dx.doi.org/10.1038/nature09022. [PubMed: 20485436]

Lourido S, Tang K, Sibley LD. Distinct signalling pathways control *Toxoplasma* egress and host-cell invasion. EMBO J. 2012; 31:4524–4534. [PubMed: 23149386]

MacKay RJ. Equine Protozoal Myeloencephalitis: Treatment, Prognosis, and Prevention. Clin Tech Equine Pract. 2006; 5:9–16.

Mackay RJ, Tanhauser ST, Gillis KD, Mayhew IG, Kennedy TJ. Effect of intermittent oral administration of ponazuril on experimental *Sarcocystis neurona* infection of horses. Am J Vet Res. 2008; 69:396–402. [PubMed: 18312139]

Marr CM, Reef VB, Reimer JM, Sweeney RW, Reid SW. An echocardiographic study of atrial fibrillation in horses: before and after conversion to sinus rhythm. J Vet Intern Med. 1995; 9:336–340. [PubMed: 8531180]

Martinez Molina D, Jafari R, Ignatushchenko M, Seki T, Larsson EA, Dan C, Sreekumar L, Cao Y, Nordlund P. Monitoring drug target engagement in cells and tissues using the cellular thermal shift assay. Science. 2013; 341:84–87. [PubMed: 23828940]

McClure SR, Palma KG. Treatment of equine protozoal myeloencephalitis with nitazoxanide. J. Equine Vet Science. 1999; 19:639–641.

Murphy RC, Ojo KK, Larson ET, Castellanos-Gonzalez A, Perera BG, Keyloun KR, Kim JE, Bhandari JG, Muller NR, Verlinde CL, White AC, Merritt EA, Van Voorhis WC, Maly DJ. Discovery of Potent and Selective Inhibitors of Calcium-Dependent Protein Kinase 1 (CDPK1) from *C. parvum* and *T. gondii* . ACS Med Chem Lett. 2010; 1:331–335. [PubMed: 21116453]

Ojo KK, Larson ET, Keyloun KR, Castaneda LJ, DeRocher AE, Inampudi KK, Kim JE, Arakaki TL, Murphy RC, Zhang L, Napuli AJ, Maly DJ, Verlinde C, Buckner FS, Parsons M, Hol WGJ, Merritt EA, Van Voorhis WC. *Toxoplasma gondii* calcium-dependent protein kinase 1 is a target for selective kinase inhibitors. Nature Struct. Mol. Biol. 2010; 17:602–607. [PubMed: 20436472]

Ojo KK, Arakaki TL, Napuli AJ, Inampudi KK, Keyloun KR, Zhang L, Hol WG, Verlinde CL, Merritt EA, Van Voorhis WC. Structure determination of glycogen synthase kinase-3 from *Leishmania major* and comparative inhibitor structure-activity relationships with *Trypanosoma brucei* GSK-3. Mol Biochem Parasitol. 2011; 176:98–108. [PubMed: 21195115]

Ojo KK, Eastman RT, Vidadala R, Zhang Z, Rivas KL, Choi R, Lutz JD, Reid MC, Fox AM, Hulverson MA, Kennedy M, Isoherranen N, Kim LM, Comess KM, Kempf DJ, Verlinde CL, Su XZ, Kappe S, Maly DJ, Fan E, Van Voorhis WC. A specific inhibitor of PfCDPK4 blocks malaria transmission: Chemical-genetic validation. J Infect Dis. 2014a; 20:275–284.

Ojo KK, Reid MC, Kallur Siddaramaiah L, Müller J, Winzer P, Zhang Z, Keyloun KR, Vidadala RS, Merritt EA, Hol WG, Maly DJ, Fan E, Van Voorhis WC, Hemphill A. *Neospora caninum* calcium-dependent protein kinase 1 is an effective drug target for neosporosis therapy. PLoS One. 2014b; 9:e92929. [PubMed: 24681759]

Pollard CE, Abi Gerges N, Bridgland-Taylor MH, Easter A, Hammond TG, Valentin JP. An introduction to QT interval prolongation and non-clinical approaches to assessing and reducing risk. Br J Pharmacol. 2010; 159:12–21. [PubMed: 20141516]

Studier FW. Protein production by auto-induction in high density shaking cultures. Protein Expr Purif. 2005; 41:207–234. [PubMed: 15915565]

Vidadala RS, Rivas KL, Ojo KK, Hulverson MA, Zambriski JA, Bruzual I, Schultz TL, Huang W, Zhang Z, Scheele S, DeRocher AE, Choi R, Barrett LK, Siddaramaiah LK, Hol WG, Fan E, Merritt EA, Parsons M, Freiberg G, Marsh K, Kempf DJ, Carruthers VB, Isoherranen N, Doggett JS, Van Voorhis WC, Maly DJ. Development of an Orally Available and Central Nervous System (CNS) Penetrant *Toxoplasma gondii* Calcium-Dependent Protein Kinase 1 (TgCDPK1) Inhibitor with Minimal Human Ether-a-go-go-Related Gene (hERG) Activity for the Treatment of Toxoplasmosis. J Med Chem. 2016; 59:6531–6546. [PubMed: 27309760]

Wernimont AK, Artz JD, Finerty P Jr, Lin YH, Amani M, Allali-Hassani A, Senisterra G, Vedadi M, Tempel W, Mackenzie F, Chau I, Lourido S, Sibley LD, Hui R. Structures of apicomplexan calcium-dependent protein kinases reveal mechanism of activation by calcium. Nat Struct Mol Biol. 2010; 17:596–601. [PubMed: 20436473]

Yeargan M, de Assis Rocha I, Morrow J, Graves A, Reed SM, Howe DK. A new trivalent SnSAG surface antigen chimera for efficient detection of antibodies against *Sarcocystis neurona* and diagnosis of equine protozoal myeloencephalitis. J Vet Diagn Invest. 2015; 27:377–381. [PubMed: 25943129]

Highlights

- *Sarcocystis neurona (Sn)*CDPK1 has an atypical small gatekeeper residue selectively inhibited by BKIs.

- Evidence is provided that shows *Sn*CDPK1 is a potential target for rational EPM drug development.

- Bumped kinase inhibitors interfered with an early step in *S. neurona* tachyzoite host cell invasion.

- Nine of 10 mice in a BKI-1553 experimentally treated group were cured of Equine Protozoal Myeloencephalitis.

```
SnCDPK1   50 FVQHSTAVFSDRYKGQRVLGKGSFGEVILCKDKITGQECAVKVISKRQVKQKTDKESLLREVQLLKQLDHPNIMKLYEIF  129
TgCDPK1   39 FVQHSTAVFSDRYKGQRVLGKGSFGEVILCKDKITGQECAVKVISKRQVKQKTDKESLLREVQLLKQLDHPNIMKLYEFF  118


SnCDPK1  130 EDRGYYYLVGEVYCGGELFDEIISRKRFSEVDAARIIRQVLSGITYMHKNKVVHRDLKPENLLLESKSKDANIRIIDFGL  209
TgCDPK1  119 EDKGYFYLVGEVYTGGELFDEIISRKRFSEVDAARIIRQVLSGITYMHKNKIVHRDLKPENLLLESKSKDANIRIIDFGL  198
```
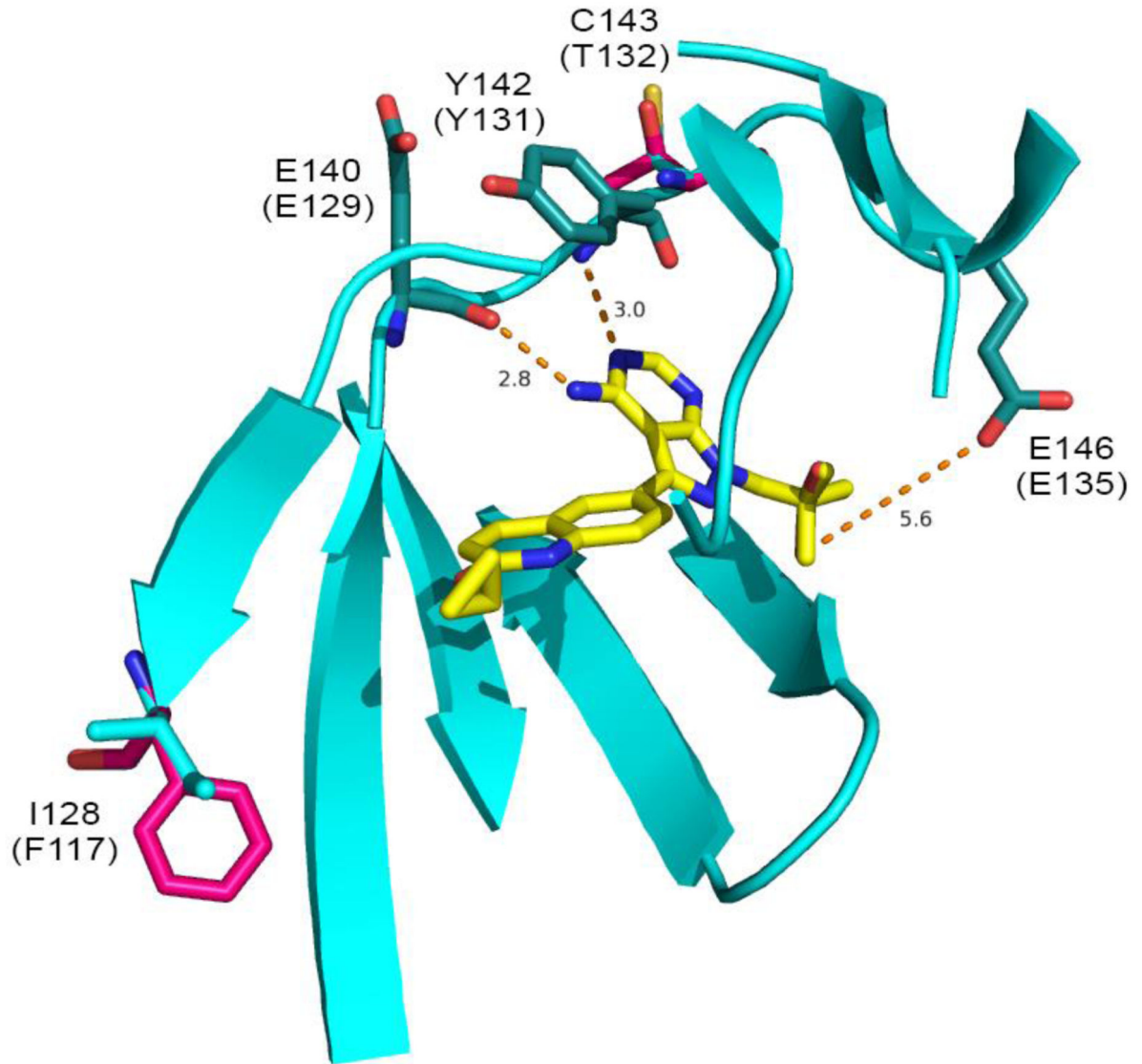

Fig. 1.
Alignment of amino acid residues of *Toxoplasma gondii* calcium-dependent protein kinase 1 (*Tg*CDPK1) and the *Sarcocystis neurona (Sn)*CDPK1 homolog. Hypothetical homology model of *Sn*CDPK1 superimposed on *Tg*CDPK1-1561 crystal complex (PDB accession code: **4TZR**) showing the spatial orientation and interaction of active site residues shown in boxes with the bumped kinase inhibitor (BKI). Red colored amino acid letters represent those residues that are not part of the ATP binding domain (Ojo et al., 2010). The model showed similar hydrogen-bonding of the backbone carbonyl of E140 (E129) and the

secondary amine of Y142 (Y131) to the exocyclic amine and adjacent endocyclic nitrogen of the pyrazolopyrimidine ring of 1561. The 2-methylpropan-2-ol R2 group extends into the ribose pocket in the kinase active site and made a hydrogen bond with E146 (E135) side chain carboxylate.
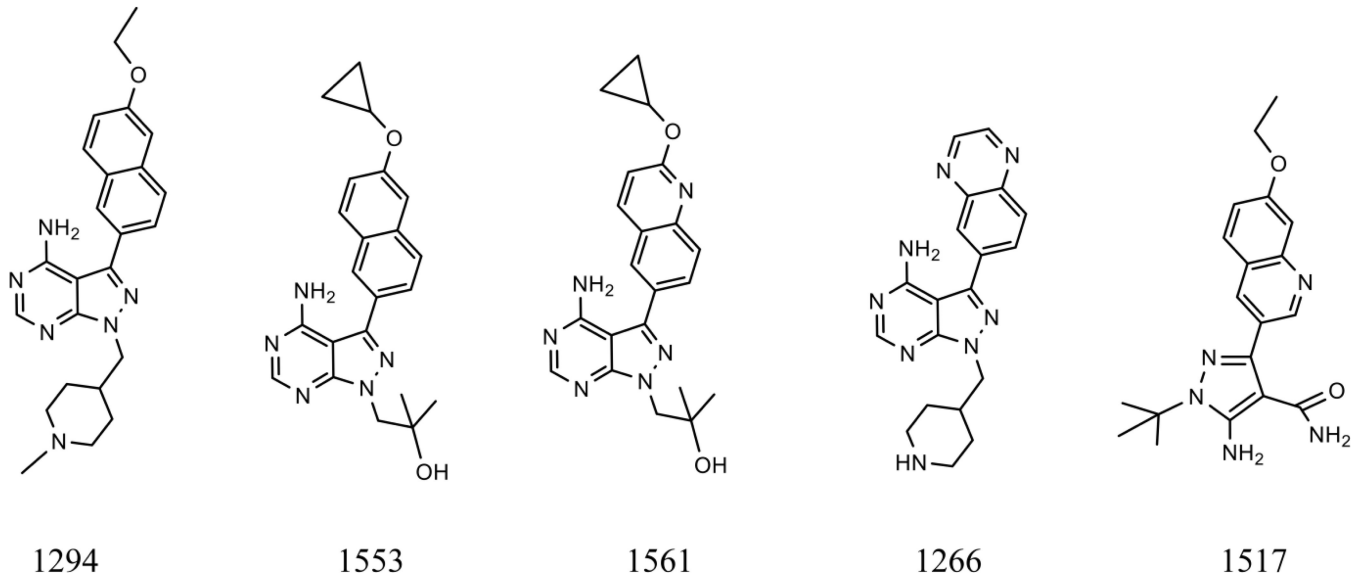
Fig. 2.
Bumped kinase inhibitor (BKI) structures. Chemical structures showing the similarities and differences between the pyrazolopyrimidine scaffold of BKIs (1266, 1294, 1553 and 1561) and the 5-Aminopyrazole-4-carboxamide scaffold represented by 1517.
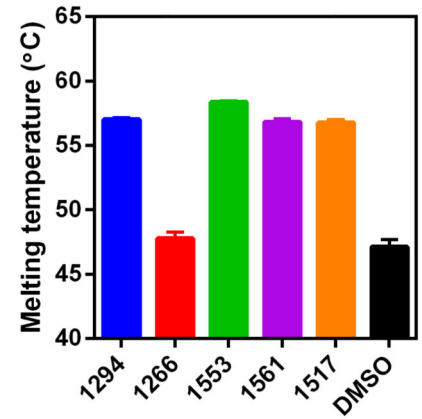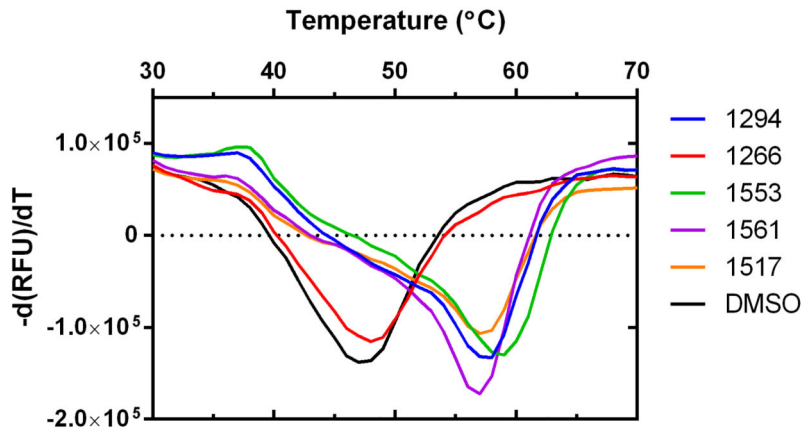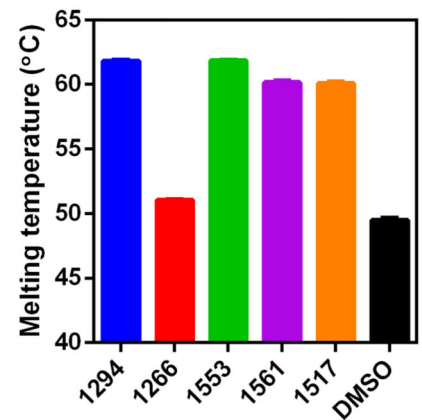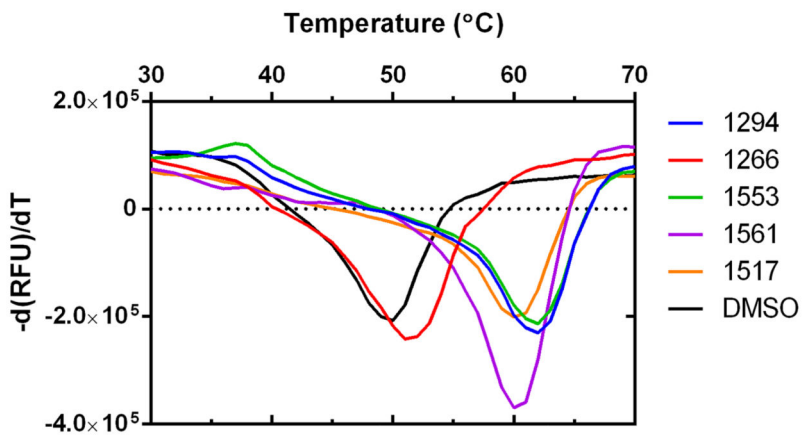
Fig. 3.
Recombinant protein thermal shift data. (A) *Sarcocystis neurona* calcium-dependent protein kinase 1 (*Sn*CDPK1) and (B) *Toxoplasma gondii (Tg)*CDPK1 enzymes showing thermal stabilization of recombinant proteins in the presence of 20 μM bumped kinase inhibitor (BKI) and 5% DMSO final concentration. Changes in melting temperature (T_m) were determined from comparative derivative plots of BKI analogues relative to the no compound DMSO controls.
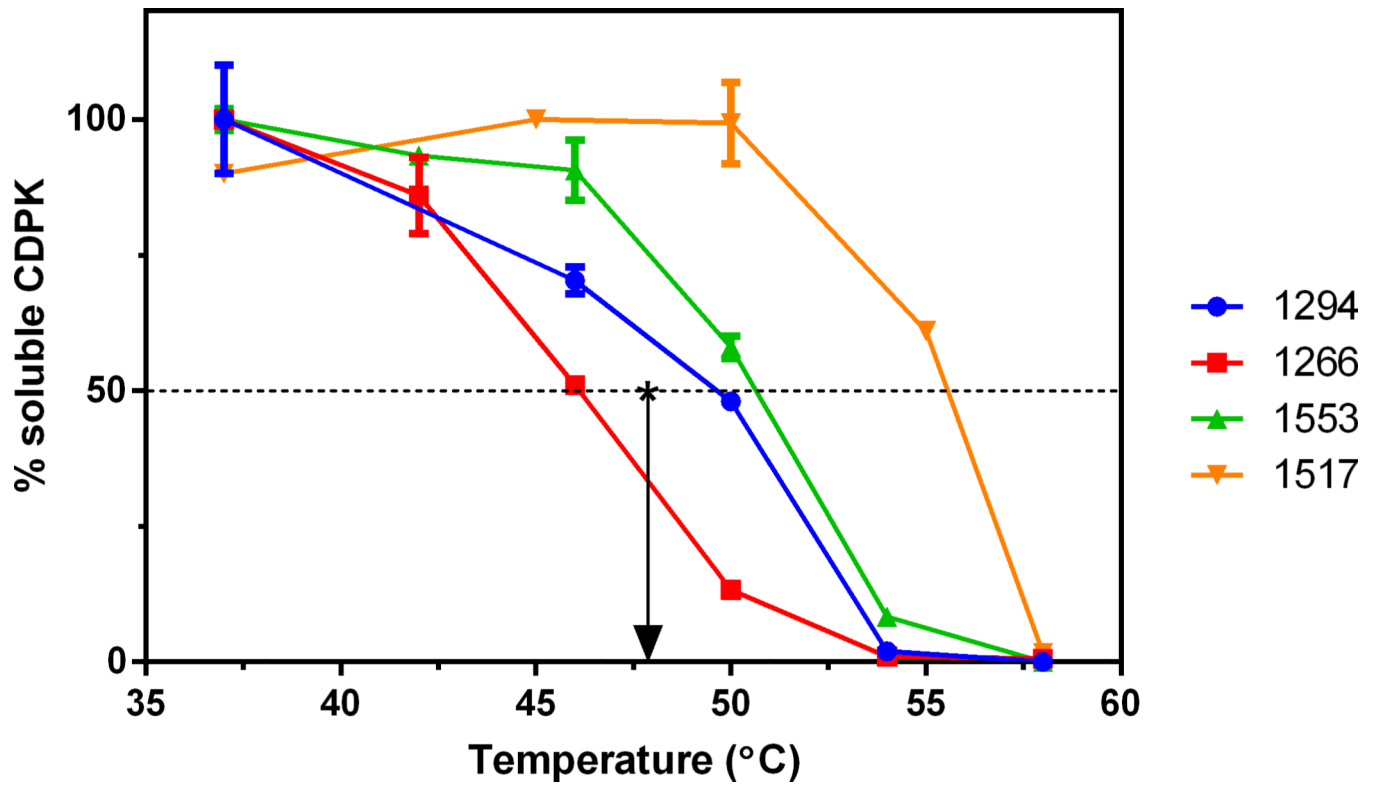
Fig. 4.
Cell lysate thermal denaturation plots. Percentage of soluble *Sarcocystis neurona* calcium-dependent protein kinase 1 (*Sn*CDPK1) remaining in lysates, compared with unheated controls, after exposure to the temperatures shown, centrifugation, and western blotting with anti-*Toxoplasma gondii (Tg)*CDPK1. The *arrow marks the melting temperature (T_m) of no compound (DMSO only) control.
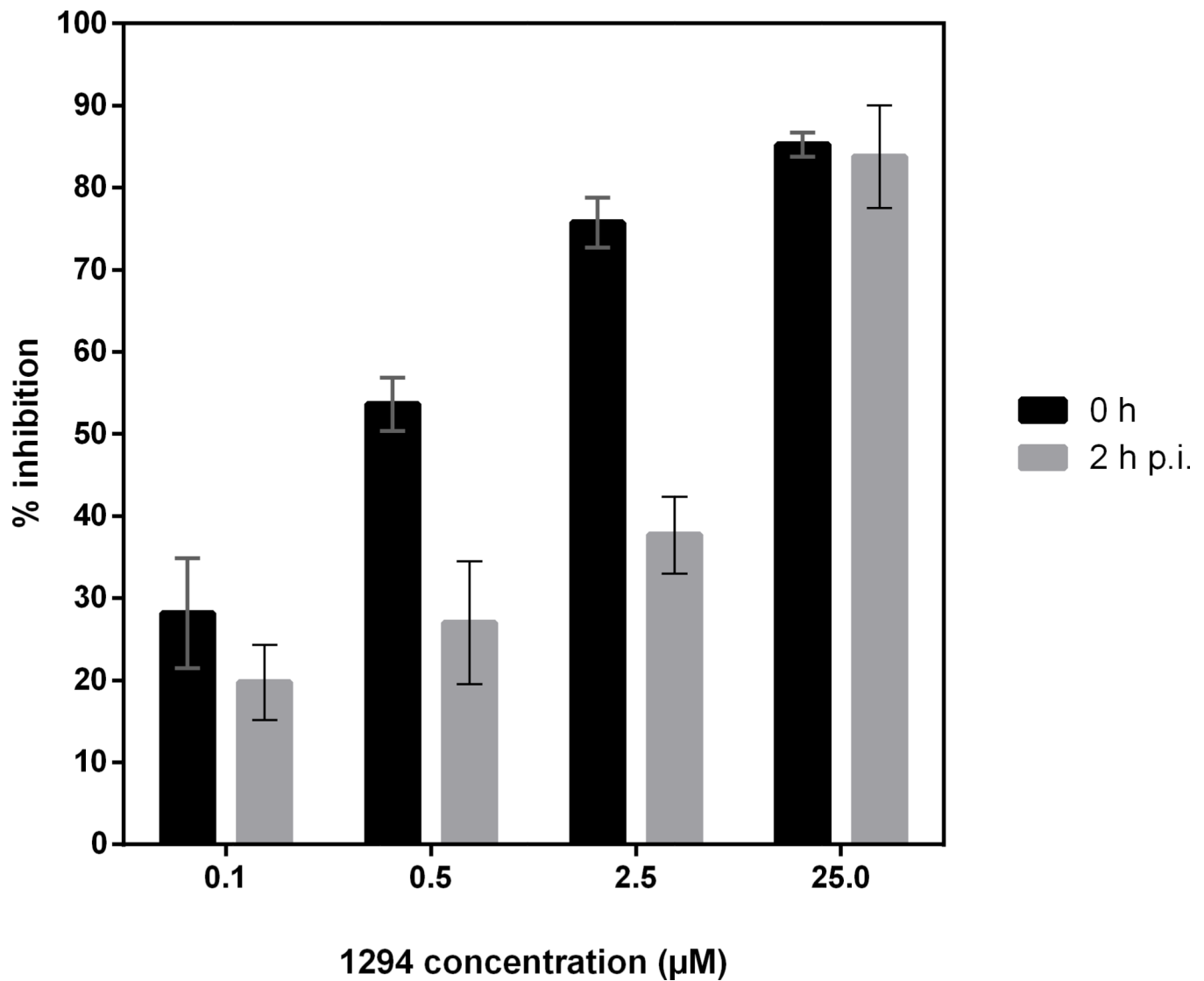
Fig. 5.
Bumped kinase inhibitor (BKI) 1294 is more effective if added at the time of infection rather than 2 h later. Culture-derived merozoites (4×10^4/well) of *Sarcocystis neurona*-yellow fluorescent protein (YFP) clone F9F seeded onto 96-well monolayers of bovine turbinate (BT) host cells. BKI-1294 was added at the time of parasite inoculation (0 h) and incubated for 2 h. For the second part of the experiment, BKI-1294 was added 2 h p.i.. Wells were washed two times to remove non-invaded *S. neurona* before adding BKI-1294 back to wells. Plates were incubated at 37°C for 4 days, and fluorescence measured growth inhibition was based on *S. neurona*-YFP control wells containing no drug. BT cells in 2% serum were used as blank wells. The data above represents the mean of eight wells.

Table 1

Sarcocystis neurona calcium-dependent protein kinase 1 (*Sn*CDPK1) cell lysate thermal shift and enzyme inhibition with *S. neurona* cell EC$_{50}$s in the presence of bumped kinase inhibitors (BKIs).

BKIs	Recombinant *Sn*CDPK1 Thermal Shift (°C) at 20 µM	Recombinant *Tg*CDPK1 Thermal Shift (°C) at 20 µM	*S. neurona* cell CDPK1 Thermal Stability (°C)	*Sn*CDPK1 enzyme IC$_{50}$ (µM)	*Tg*CDPK1 enzyme IC$_{50}$ (µM)	*S. neurona* cell growth EC$_{50}$ (µM)
1553	11.2	12.3	4.1	0.009	0.001[a]	0.042
1266	0.7	1.6	0	>2	0.500[b]	>10
1294	9.9	12.3	2.7	0.006	0.003[c]	0.068
1561	9.6	10.6	ND	0.008	0.002[a]	0.128
1517	9.6	10.5	8.0	0.002	0.002[d]	0.042

[a] Vidadala et al., 2016

[b] Ojo et al., 2012

[c] Johnson et al., 2012

[d] Huang et al., 2015

Tg, *Toxoplasma gondii*; IC$_{50}$, inhibition concentration to give 50% reduction in enzyme activity; ND, not done; EC$_{50}$, inhibition concentration to give 50% reduction in cell growth.

Table 2

Sarcocystis neurona infection in IFNγ-knock out (KO) mice and evaluation of anti-parasitic efficacy of bumped kinase inhibitor BKI-1553.

Group No., sex (number of animals)	Group detail	Infection[a]	Dosing (d.p.i.)	Clinical signs[c]	Necropsy (d.p.i.)	Diagnosis Serology (reciprocal end-point titers)	Histology	Sub-inoculation
#1, M(*n*=5)	Age match	No	No	No	31	ND	Negative	
#2, F(*n*=5)	control	No	No	No	54	Negative (<250)	Negative	
#3, M(*n*=5)	Infection	Yes	No	Yes	41–45	Positive (>8000)	Positive	
#4, F(*n*=5)	control	Yes	No	Yes	39–70	Positive (>8000)	Positive	
#5, M(*n*=5)	Drug control	No	Yes (1–30)	No	31	ND	Negative	
#6, F(*n*=5)		No	Yes (1–30)	No	54	Negative (<250)	Negative	
#7, M(*n*=5)	Experimental	Yes	Yes (1–30)	No	70	Negative[d] (<250)	Negative[e]	Positive[f]
#8, F(*n*=5)	group	Yes	Yes (1–30)	No	70	Negative[d] (<250)	Negative	Negative[f]

[a] *Sarcocystis neurona* strain SN37 cell cultured merozoites (20,000 parasites/animal/0.5 mL) were inoculated s.c.

[b] BKI-1553 dissolved in water with 0.5% saccharine, offered as drinking water on the day after infection and continued for 30 days. Estimated dose was 4.8 mg/kg/day/oral.

[c] Weak, hunching, neurological signs.

[d] One mouse each from groups #7 and #8 was seropositive, with reciprocal end-point titers of 2000 and 1000, respectively.

[e] One mouse in group #7 was found to have parasites in the brain at autopsy, the other four did not.

[f] Sub-inoculation of pooled brains of group #7 mice resulted in *S. neurona* infection. Sub-inoculation of pooled brains of group #8 was negative for *S. neurona* infection.

M, male; F, female; ND, not done; d.p.i., days p.i.

Table 3

Bumped kinase inhibitor (BKI)-1553 blood levels of infected and treated mice from groups #7 and #8 during continuous dosing in drinking water (mean value was 6.0 μM). These blood samples were taken midway through the study which suggests a steady state phase. One mouse (F) with a measured blood level of 5.79 μM was found to have parasites in the brain by immunohistological examination. The mouse did not show any clinical manifestation of the disease.

Time of sample collection	Mouse ID and Plasma Concentration (μM)									
	A	B	C	D	E	F	G	H	I	J
Evening	5.03	8.28	9.9	6.08	6.93	ND	ND	ND	ND	ND
Morning	6.78	4.54	8.34	5.69	4.88	5.79	3.62	6.18	2.48	4.6

ND, not done.